

Merger history of dark matter halos in the light of H_0 tension

Hamed Kameli and Shant Baghram [★]

Department of Physics, Sharif University of Technology, P. O. Box 11155-9161, Tehran, Iran

Accepted XXX. Received YYY; in original form ZZZ

ABSTRACT

The Hubble tension may introduce a new course of action to revise the standard Λ CDM model to unravel dark energy and dark matter physics. The Hubble parameter can be reconstructed by late-time observations of the background evolution model independently to reconcile the Hubble tension. We relate the reconstructed Hubble parameter to the structure formation and large scale structure observables in this work. We use the excursion set theory to calculate the number density of dark matter halos, the distribution of sub-halo progenitors, and dark matter halos' merger rate. We obtain the results for both the Markov and non-Markov extension of the excursion set theory. We show that the number density of dark matter halos in the reconstructed model has a $\sim 2\sigma$ difference in comparison to the Planck-2018 Λ CDM in the mass range of $M < 10^{12} M_\odot$. We also compare the dark matter halo merger rate with the pair-galaxy statistics and their merger rate from observational data of HST, CANDEL survey. We assert a ~ 5 times more accurate observations in the redshift range of $z \simeq 0.75 - 2.5$ can distinguish the reconstructed model and the Planck-2018 Λ CDM.

Key words: cosmology: large-scale structure of Universe, cosmology: dark matter, galaxies: haloes

1 INTRODUCTION

It is almost more than two decades since the discovery of the accelerated expansion of the Universe with the observation of supernova type Ia (SNe Ia) Riess et al. (1998); Perlmutter et al. (1999). The standard model of cosmology known as Λ CDM emerged and withstood with most recent observations. The precise measurement of the statistics of the cosmic microwave background (CMB) radiation fluctuations enables us well to constrain the standard model parameters Aghanim et al. (2018). On the other hand, late-time observations of large scale structure (LSS), such as statistics of galaxy clustering Percival et al. (2010); Alam et al. (2017); Camacho et al. (2019) and weak lensing Hildebrandt et al. (2017) are prominent examples, which are in good agreement with the standard model. Despite all these successes, the nature of dark energy (DE), dark matter (DM), and the physics of the early Universe is still unknown Bull et al. (2016). One possible way to address these fundamental questions is to focus on the data and theory's known tensions through new ideas Peebles (2014). One of the main tensions comes from the measurement of the Hubble constant H_0 . The H_0 obtained from local standard candles has

almost $\sim 4.4\sigma$ difference with the CMB data Riess et al. (2019) ¹. This discrepancy could result from a statistical fluke, observational systematics, or a hint to a new physics. In this direction, many proposals have been introduced, such as early time modification of sound horizon Poulin et al. (2019), late time DE models Di Valentino et al. (2020), interacting DE-DM models Di Valentino et al. (2020), and modified gravity theories Khosravi et al. (2019). Obviously, a new physics proposed to solve the Hubble tension should also be consistent with other cosmological observations. The LSS observations are important to study beyond standard Λ CDM models Hildebrandt et al. (2006); Pogosian & Silvestri (2008); Baghram & Rahvar (2008); Baghram et al. (2009); Baghram & Rahvar (2010, 2014); Koyama (2016); Klypin et al. (2019).

In this work, we suggest testing the effect of the background evolution of the late time Universe, encoded in the Hubble parameter, on the LSS observations. We study the effect of this modified Hubble parameter on the matter power spectrum, number density, and the merger history of DM halos.

¹ $H_0 = 74.03 \pm 1.42 \text{ km s}^{-1} \text{ Mpc}^{-1}$ from local measurement Riess et al. (2019) and $H_0 = 67.27 \pm 0.60 \text{ km s}^{-1} \text{ Mpc}^{-1}$ from Planck-2018 data Aghanim et al. (2018)

[★] baghram@sharif.edu

We show that the modified Hubble parameter has observable effects on DM halos' statistics in the context of hierarchical structure formation. The modification in the merger history of DM halos can be considered as a new proposal to address the questions and caveats in structure formation such as the seeds of supermassive black holes [Heckman & Best \(2014\)](#), the quenching of massive galaxies [Man & Belli \(2018\)](#) and the observation of flat galaxies [Peebles \(2020\)](#).

The structure of this work is as below: In [Sec.2](#), we review the theoretical background of this work, specially the excursion set theory (EST) and the LSS observations in linear and non-linear scales. In [Sec.3](#), we discuss our results and implications of reconstructed Hubble parameter (obtained from [Wang et al. \(2018\)](#)) in LSS observables and finally in [Sec.4](#) we conclude and propose the future remarks. The results for flat Λ CDM model are based on Planck-2018 with matter density of $\Omega_m = 0.27$, the $H_0 = 67 \text{ km s}^{-1} \text{ Mpc}^{-1}$ and $n_s = 0.96$ [Aghanim et al. \(2018\)](#).

2 THEORETICAL BACKGROUND: FROM HUBBLE PARAMETER TO LSS OBSERVABLES

This section reviews the theoretical background of this work, which shows the effect of the Hubble parameter on DM halos formation history and LSS observables such as halos number density and merger rate. First, we discuss the linear theory in the standard model. Then the non-linear structure formation of DM halos is discussed in the context of EST. Finally, we review the recent implications of the non-Markov EST model and the numerical counting methods to obtain the halos number density and their merger history.

Linear theory

To study the linear structure formation, we use the perturbed Friedmann Lemaitre Robertson Walker (FLRW) metric

$$ds^2 = a^2(\eta) \left[-(1 + 2\Psi(t, \vec{x}))d\eta^2 + (1 + 2\Phi(t, \vec{x}))dx^i dx^j \delta_{ij} \right], \quad (1)$$

where η is the conformal time, Ψ is the Newtonian potential and Φ is the curvature perturbation. Using the Einstein's equations we have relativistic Poisson equation [Amendola \(2004\)](#)

$$k^2 \Phi(k, z) = 4\pi G(1+z)^{-2} \bar{\rho}(z) \left[\delta(k, z) + \frac{3\mathcal{H}(1+w)\theta(k, z)}{k^2} \right], \quad (2)$$

where $\bar{\rho}$ is the mean matter density, $\delta = \rho/\bar{\rho} - 1$ is density contrast and $\theta = ikv_k$ is the peculiar velocity's divergence in Fourier space. Note that \mathcal{H} is the conformal Hubble parameter and $w = P/\rho$ is pressure to density ratio (we set $w=0$ as we deal with non-relativistic DM). The continuity and Euler equations for cold DM raised from energy-momentum conservation are

$$\delta' = -\theta - 3\Phi', \quad (3)$$

$$\theta' + \mathcal{H}\theta = k^2 \Psi. \quad (4)$$

where \prime is derivative with respect to the conformal time. Combing equations(2,3,4), we find the DM density contrast

evolution in terms of redshift in sub-horizon scales ($k \ll \mathcal{H}$) and in quasi-static regime (ignoring the time derivatives of Bardeen potentials in comparison with Hubble time scale) as

$$\frac{d^2 \delta}{dz^2} + \left[\frac{dE(z)/dz}{E(z)} - \frac{1}{1+z} \right] \frac{d\delta}{dz} - \frac{3}{2} \Omega_m \frac{1+z}{E^2(z)} \delta = 0, \quad (5)$$

where $E(z) = H(z)/H_0$ is normalized Hubble parameter, Ω_m is the matter density parameter. The growth function $D(z)$ is defined as

$$\delta(z) = \frac{D(z)}{D(z=0)} \delta_{\text{ini}}, \quad (6)$$

which relates the density contrast evolution of DM to its initial value δ_{ini} . The growth function incorporates only the time evolution of the density contrast. Accordingly, the linear matter power spectrum $P_L(k, z)$ will be defined as

$$P_L(k, z) = A_l k^{n_s} D^2(z) T^2(k), \quad (7)$$

where A_l is the late time amplitude of perturbations, n_s is the spectral index of the perturbations, and $T(k)$ is the transfer function. The transfer function introduces the scale-dependence of Bardeen potentials' evolution, considering the physics of the equality era and horizon entry. We use the Eisenstein-Hu Transfer function [Eisenstein & Hu \(1998\)](#).

Non-linear structure formation

One of the main observables in non-linear structure formation is the luminosity distribution of galaxies, which are tightly related to the number density of DM halos [Cooray & Sheth \(2002\)](#). An old but sophisticated way to calculate the number density of DM halos is the idea of Press-Schechter (PS) [Press & Schechter \(1974\)](#). PS formalism proposed that probability distribution function (PDF) of the density contrast in high redshifts, where the perturbations are almost Gaussian and linear, can be used to predict the late time number density of the DM halos. The PDF fraction of linear density contrast with a larger value than the spherical collapse barrier [Gunn & Gott \(1972\)](#) is considered the fraction of the gravitationally bound objects with the same amount of mass enclosed in the initial smoothing radius [Zentner \(2007\)](#). Later on, [Bond et al. \(1991\)](#) introduced the Excursion Set Theory (EST), which relates the statistical properties of the initial density contrast field to the number density of structures by using the stochastic process techniques. A set of trajectories is plotted in this 2 dimensional plane of density contrast versus variance. The trajectory steps are generated by smoothing window function around arbitrary points in initial density contrast field [Cooray & Sheth \(2002\)](#); [Zentner \(2007\)](#); [Nikakhtar & Baghram \(2017\)](#). The statistics of the first up-crossing from a specific barrier² of these random walk trajectories f_{FU} is related to the number density of DM halos $n(M)$ as

$$n(M)dM = \frac{\bar{\rho}}{M} f_{\text{FU}}(S) \left| \frac{dS}{dM} \right| dM, \quad (8)$$

where f_{FU} is the first up-crossing counts of density contrast variance in the interval of S and $S+dS$. The variance in each

² In more sophisticated collapse models, the barrier can be a scale dependent function [Sheth & Tormen \(2002\)](#).

smoothing scale R is obtained from the weighted integral of linear matter power spectrum as

$$S(R) = \sigma^2(R) = \frac{1}{2\pi^2} \int dk k^2 P_L(k, z=0) \tilde{W}^2(kR), \quad (9)$$

where $\tilde{W}(kR)$ is the Fourier transform of window (smoothing) function in real space.³ Bond et al. (1991) show for sharp k-space window function, the trajectories execute a random Markov walk. Accordingly, for Markovian trajectory, the analytical expression for the first up-crossing distribution is

$$f_{\text{FU}}(S, \delta_c(z)) dS = \frac{1}{\sqrt{2\pi}} \frac{\delta_c(z)}{S^{3/2}} e^{-\frac{\delta_c^2(z)}{2S}} dS, \quad (10)$$

where the redshift dependency appeared in $\delta_c(z) = \delta_c D(z=0)/D(z)$ via the growth function. It worths to mention, using other window functions, which results to non-Markov trajectories there is no analytical expression for f_{FU} . So the first up-crossing of the trajectories should be counted numerically (for more discussion see Nikakhtar et al. (2018)). In this context the merger of DM halos can be studied by conditional up-crossing. The probability of progenitor merging history of DM halo in Markov EST with mass M_1 (corresponding to variance S_1 via equation(9)) at redshift z_1 to a DM halo with a larger mass $M_2 > M_1$ (corresponding to S_2) at redshift $z_2 < z_1$ is

$$f_{\text{FU}}(S_1, \delta_1 | S_2, \delta_2) = \frac{1}{\sqrt{2\pi}} \frac{\delta_c(z_1) - \delta_c(z_2)}{(S_1 - S_2)^{3/2}} e^{-\frac{(\delta_c(z_1) - \delta_c(z_2))^2}{2(S_1 - S_2)}}. \quad (11)$$

Also, by using joint probability (note that $\delta_c(z_i) \equiv \delta_i, i = 1, 2$)

$$f_{\text{FU}}(S_2, \delta_2 | S_1, \delta_1) dS_2 = \frac{f_{\text{FU}}(S_1, \delta_1 | S_2, \delta_2) f_{\text{FU}}(S_2, \delta_2)}{f_{\text{FU}}(S_1, \delta_1)} dS_2, \quad (12)$$

we can find the merger rate probability for a halo of mass M_1 at redshift z_1 to a halo $M_2 = M_1 + \Delta M$ in $z_2 = z_1 + \Delta z$, where $\Delta z < 0$ Sheth & Tormen (1999). In other words, the conditional probability is equivalent to a merger rate probability as

$$P(\Delta M | M, z) d \ln \Delta M dz = \frac{1}{\sqrt{2\pi}} \left[\frac{S_1}{(S_1 - S_2)} \right]^{3/2} \exp\left[-\frac{\delta_c^2(S_1 - S_2)}{2S_1 S_2}\right] \times \left| \frac{d \ln \delta_c}{dz} \right| \frac{\delta_c}{\sqrt{S_2}} \left| \frac{d \ln S_2}{d \ln \Delta M} \right| dz d \ln \Delta M. \quad (13)$$

The probability of merger or mass accretion of ΔM in the Δz redshift interval is obtained from the equation(13). In Fig.1 a set of Markov trajectories are plotted in the top panel and a non-Markov set (see next subsection) in the bottom panel. We show the idea of halo formation through accretion (a smooth increase of density contrast in terms of variance) in the redshift interval of $z = 0 - 2.5$, and halo merger (a visible jump in trajectories in specified redshift for two different masses) in the upper panel.

Non-Markov extension of EST

To study DM halos' number density and their merger history, we need more realistic models and better approximations. One of the main caveats of standard EST is the use

³ We use the Gaussian filter $\tilde{W}(kR) = \exp[-(kR)^2/2]$ for non-Markov EST.

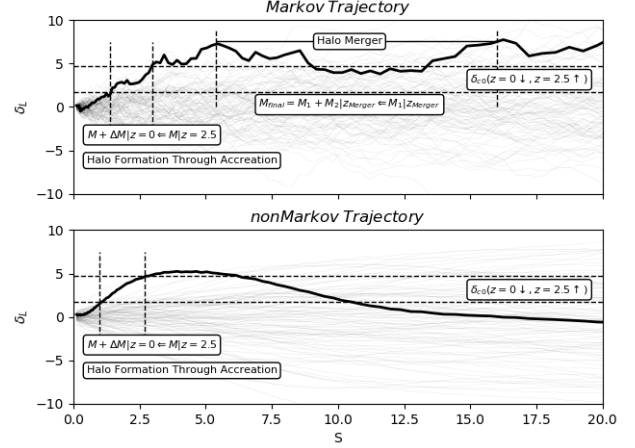


Figure 1. Top panel: A set of Markov trajectories. Bottom panel: a set of non-Markov trajectories. The idea of the halo formation and merger is depicted in the figure.

of the k-space sharp window function. If we choose more realistic smoothing functions, such as real space top-hat or Gaussian window functions (as used in this work), we end up with non-Markov trajectories. There are many attempts to address the problem of the first up-crossing in non-Markov walks. (For-example see Maggiore & Riotto (2010a,b); Musso & Sheth (2012); Musso & Sheth (2014)) We use the numerical method developed in Nikakhtar et al. (2018); Baghran et al. (2019) and it's extension to calculate number density and merger probability in Λ CDM cosmology Kameli & Baghran (2020). In non-Markov trajectories, the height of the smoothed density field extrapolated to the present time $\delta_R(\vec{x})$ is correlated to the density contrast in previous variance steps. These correlations lead to a more smoother trajectories in comparison to jagged ones in Markov case (see Fig.1), which changes the statistics of DM halos. This means that the density contrast in the n -th step can be written as

$$\delta_n = \langle \delta_n | \delta_{n-1}, \dots, \delta_1 \rangle + \sigma_{n|n-1, \dots, 1} \xi_n, \quad (14)$$

where the first term indicate that the height in n -th step of variance depends on the previous steps and ξ_n is a zero mean, unit variance Gaussian random number ($\langle \xi_n \xi_m \rangle = \delta_{nm}$). In Nikakhtar et al. (2018), a numerical method based on Cholesky decomposition is introduced to generate an ensemble of trajectories with correct statistical characteristic encoded in correlation matrix C_{ij} as

$$\langle \delta_i \delta_j \rangle \equiv C_{ij} = \int \frac{dk}{k} \frac{k^3 P_L(k)}{2\pi^2} \tilde{W}(kR_i) \tilde{W}(kR_j), \quad (15)$$

where $i(j)$ is related to the smoothing scale $R_i(R_j)$, so the statistical correlation of density contrast in different scales is embedded in C_{ij} . Then the non-Markov trajectories are obtained from

$$\delta_i = \sum_j L_{ij} \xi_j, \quad (16)$$

where L_{ij} are the components of lower triangular matrix related to the decomposed $C = \mathbf{L}\mathbf{L}^T$. Note that ξ_j , is a random number with Gaussian distribution. By using a proper power spectrum in equation(15), we can use the Cholesky

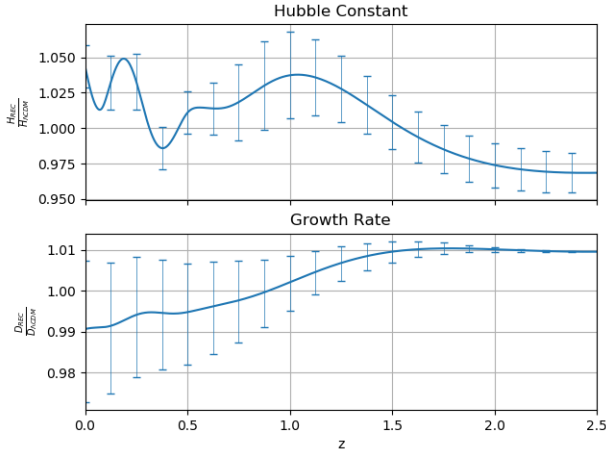


Figure 2. Top panel: the reconstructed Hubble parameter normalized to Planck-2018 Λ CDM is plotted versus redshift. The data used in the reconstructed model are SNe Type Ia, BAO and Planck distance indicator (see the main text for the references). The error-bars are the 1σ confidence level of the reconstructed Hubble parameter. Bottom panel: the ratio of the growth rate of the reconstructed model to Λ CDM prediction.

decomposition method to produce cosmological model dependent trajectories. In the next section, we will use the Cholesky method to produce the trajectories with the standard Planck-2018 Λ CDM and the reconstructed Hubble parameter model.

3 RESULTS: FROM RECONSTRUCTED HUBBLE PARAMETER TO MERGER HISTORY

In this section, we present our results on the effect of the reconstructed Hubble parameters on the LSS observables, and we compare them with standard Planck-2018 Λ CDM predictions. We use the late time distance indicator observations to reconstruct the Hubble parameter, independent of any proposed cosmological model introduced in Wang et al. (2018). The background data used for Hubble reconstruction are supernovae data from joint light analysis (JLA) sample Betoule et al. (2014), baryonic acoustic oscillation (BAO) measurements from 6dF Galaxy Survey (6dFGS) Betoule et al. (2011), SDSS DR7 Main Galaxy Sample (MGS) Riess et al. (2015), tomographic BOSS DR12 (TomoBAO) Wang et al. (2017), eBOSS DR14 quasar sample (DR14Q) Ata et al. (2018) and the Lyman- α forest of BOSS DR11 quasars Font-Ribera A. et al. (2014); Delubac et al. (2015). In Fig.2 top panel, the reconstructed Hubble parameter normalized to the Planck-2018 Λ CDM is plotted Wang et al. (2018). The modified growth function is extracted by equation(5) using the reconstructed Hubble parameter. The reconstructed growth function ratio to the Planck-2018 Λ CDM is plotted in Fig.2 bottom panel. It is worth to mention that in the context of the non-linear structure formation and EST, modified growth function can affect the matter distribution. This modification results from the variation of the redshift dependency of the barrier $\delta_c(z)$. Accordingly, the first up-crossing and conditional one (equations(10) and (11)) will be changed due to modified barrier δ_c . In this direction, we

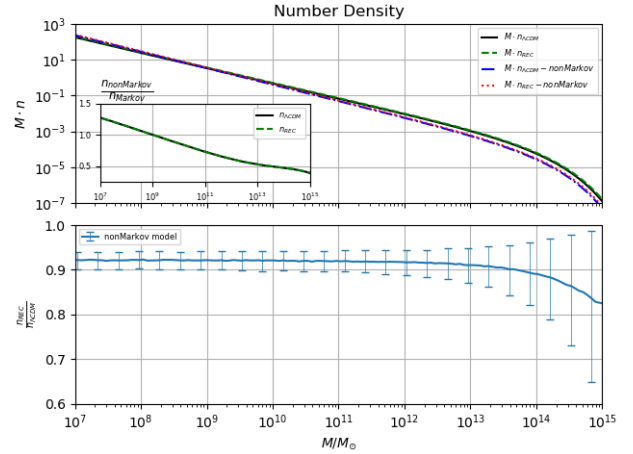


Figure 3. Top panel: the number density of dark matter halos is plotted for standard Planck-2018 Λ CDM and reconstructed model. Bottom panel: the ratio of the number density in two models is plotted versus redshift.

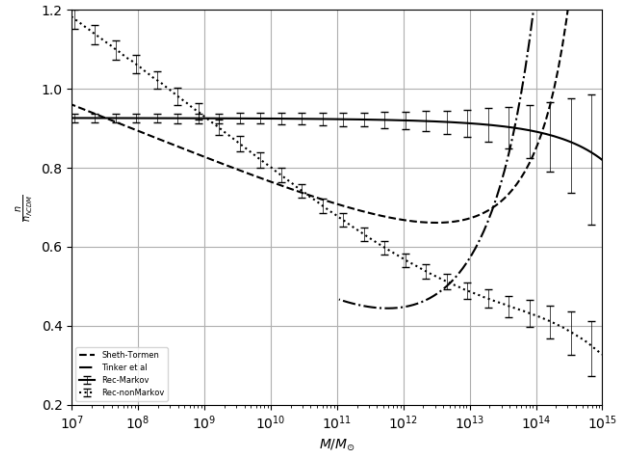


Figure 4. The ratio of DM halos' number density in the reconstructed model (Markov and non-Markov) and simulation-based fitting functions to Planck-2018 Λ CDM Markov case.

study the statistics of DM halos in both models. In Fig.3, we show the number density of DM halos in two models for both Markov and non-Markov EST extension. The bottom panel shows the number density ratio in reconstructed and Planck-2018 Λ CDM model in non-Markov extension. The error-bars introduced due to the reconstruction method is small enough to distinguish the two models by their DM halo number density prediction in almost $\sim 2\sigma$ in DM halo mass ranges $M < 10^{12} M_\odot$. In Fig.4, we compare the number density of DM halos in the reconstructed model (Markov and non-Markov) and simulation-based fitting functions (Sheth-Tormen Sheth & Tormen (1999) and Tinker et al. model Tinker et al. (2008)) to Planck-2018 Λ CDM Markov as the most basic analytical predicted DM number density. For interpreting the Fig.4, we should take into account the moving barrier of the critical density $\delta_c = \delta_c(S)$ Sheth & Tormen (2002). Also, the scope of the validity of our assumption, which relates the first up-crossing statistics to the DM halo number density straightforwardly, must be reconsidered. In this

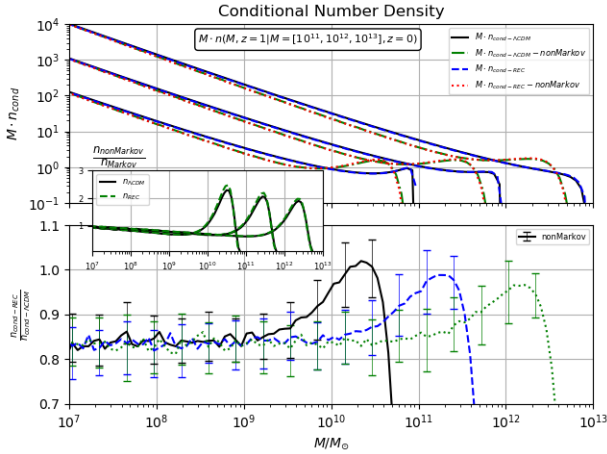


Figure 5. Top panel: the mass function of DM sub-halos (progenitors) in redshift $z = 1$, which will merge to form halos with masses $10^{11}, 10^{12}, 10^{13} M_\odot$ in present time $z = 0$. Bottom panel: the ratio of conditional mass function predicted by reconstructed model to Planck-2018 Λ CDM Markov model. Inset figure: the ratio of the non-Markov to Markov is plotted for each model independently.

direction, ideas such as peak theory [Bardeen et al. \(1986\)](#) and, more recently, the excursion set theory of peaks has been introduced [Paranjape & Sheth \(2012\)](#). Furthermore, to compare our results with observational data, we should consider all the complications raised from the halo occupation distribution physics [Mo et al. \(2010\)](#). That leads us to predict an observable change in galaxies’ luminosity function compared to the standard model. To overcome this obstacle, we suggest that DM halos’ merger rate can be related to an observational quantity such as pairing fraction of the galaxies [Duncan et al. \(2019\)](#). One important quantity, related to merger history is the progenitor distribution of DM halos. In [Fig.5](#), we plot the mass function of DM sub-halos (progenitors) in redshift $z = 1$, which will merge to form halos with masses $10^{11}, 10^{12}, 10^{13} M_\odot$ in present time $z = 0$ (see equation(11)). The bottom panel of [Fig.5](#) shows the ratio of conditional mass function predicted by the reconstructed model to the Planck-2018 Λ CDM Markov model. The inset figure shows the ratio of the non-Markov to Markov for each model independently. The theoretical uncertainty of progenitor mass distribution predicted by the reconstructed model is low enough for two models to distinguish them with more than $\sim 2\sigma$ confidence level. In [Fig.6](#) top panel, we plot the merger rate for a DM halo of $M = 10^{11} M_\odot$ with another halo with mass ΔM . The merger process is occurred in the redshift interval of $z = (0.75-1.25)$ to form a DM halo with mass $M_f = M + \Delta M$, where the mass range is $\log_{10} \Delta M/M = [-1, 1]$. In the bottom panel of [Fig.6](#), the ratio of merger rate in reconstructed model to Planck-2018 Λ CDM Markov case is plotted. This ratio is almost the same in both Markov and non-Markov cases. However, the absolute values are different due to the memory dependence of the non-Markov case, which decreases the number of jagged jumps and mergers compared to the Markov case (see [Fig.1](#)). This effect can be the subject of a study in future work. In a recent work by [Duncan et al. \(2019\)](#), a study is done to find the ma-

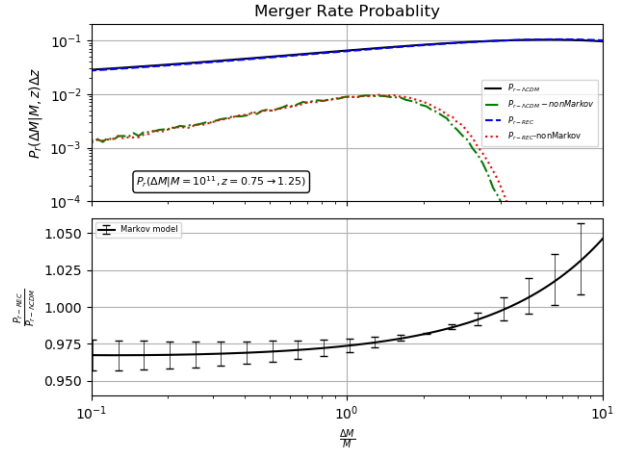


Figure 6. Top panel: the merger rate for a DM halo of $M = 10^{11} M_\odot$ with another halo with mass ΔM . Bottom panel: the ratio of merger rate in reconstructed model to Planck-2018 Λ CDM Markov model.

ior merger rate⁴ of galaxies in the Hubble Space Telescope (HST) Cosmic Assembly Near-infrared Deep Extragalactic Legacy Survey (CANDELS). The idea is based on counting the pair galaxies in redshift bins up to $z \simeq 6.5$. The galaxies distance separation in the interval of $r \simeq (5-30)$ kpc and redshift or velocity separation of $\Delta v \leq 500 \text{ km s}^{-1}$ are considered as candidates for merging. The quantity $f_{\text{pair}} = (\text{Number of pair galaxies})/(\text{Number of total galaxies})$ is defined respectively. By the knowledge of merging time scale $\tau_p = 2.4 \times (1+z)^{-2} \text{ Gyr}$, the merger rate of galaxies are obtained and reported for two stellar mass range $9.7 < \log M_*/M_\odot < 10.3$ and $\log M_*/M_\odot > 10.3$ in Table 5 of [Duncan et al. \(2019\)](#). If we assume a constant mass to light ratio (i.e $M_*/M = 0.1$) for the pairing galaxies, we can use this results to compare with DM halo merger rate. In [Fig.7](#), we plot the merger rate ratio of DM halos for the reconstructed model to the Planck-2018 Λ CDM Markov case versus redshift. This ratio is plotted for $\Delta M/M = 1/4$ and stellar Mass $M_* = 10^{10} M_\odot$ in the top panel and $M_* = 10^{11} M_\odot$ in the bottom panel (see equation(13)). The blue dash-dotted lines show the error-bar on the merger rate based on Table 5 of [Duncan et al. \(2019\)](#). The green dotted lines show an optimistic future prediction (~ 5 times more accurate than the realistic errors) to decrease the error bars on the merger rate in the redshift range of $z \simeq 0.75-2.5$. That can be done by increasing the precision of the observations with better photometric and spectroscopic measurements. Also, the improvement can be achieved by increasing the statistics of galaxies by future LSS surveys. We assert that one can distinguish the standard Λ CDM from the reconstructed model by future observations. We obtain all results for a model-independent case, and it can be easily applied to any other cosmological model, which has affected the Hubble parameter.

⁴ Mass ratio of the major merger is in the range of $> 1/4$

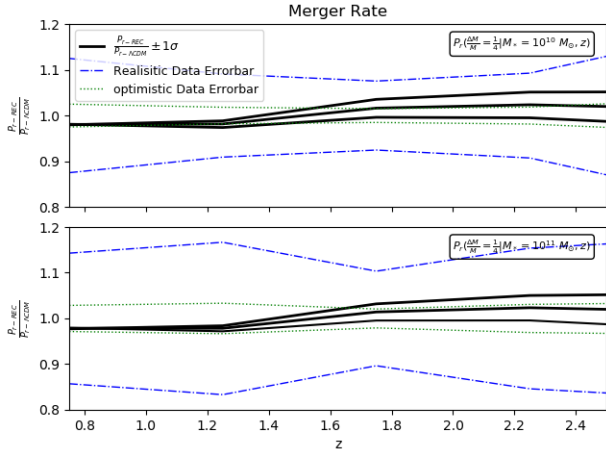


Figure 7. The merger rate ratio of DM halos for the reconstructed model to the Planck-2018 Λ CDM Markov case is plotted versus redshift. This ratio is plotted for $\Delta M/M = 1/4$ and stellar Mass $M_* = 10^{10} M_\odot$ in the top panel and $M_* = 10^{11} M_\odot$ in the bottom panel.

4 CONCLUSION AND FUTURE REMARKS

The standard cosmological model known as Λ CDM is very successful in describing different observations from CMB to the galaxies’ distribution in the late time. However, there are observational and theoretical tensions, which may introduce new venues to go beyond the standard model and shed light on the physics of dark energy, dark matter, and the early Universe. The H_0 tension is one of the most challenging and discussed problems in recent years. In this work, we use a model-independent reconstructed Hubble parameter based on late time background observational data (i.e., SNe Ia, BAO, CMB distance indicator, and Hubble constant from local measurements), as an alternative to Λ CDM. Based on this model, we calculate the LSS observables, such as the number density of DM halos, the probability distribution of DM progenitors, and the merger rate. We compare the results with the Planck-2018 Λ CDM. This procedure’s idea is that the LSS observables in non-linear scales can be used as a further criterion to distinguish the models, which could reconcile the Hubble tension. We are interested in the merger history of dark matter halos as the hierarchical structure formation’s backbone.

We show that the error-bars of the reconstructed model is small enough to distinguish the two models by their DM halo number density prediction in almost $\sim 2\sigma$ in DM halo mass ranges $M < 10^{12} M_\odot$. Also, the theoretical uncertainty of progenitor mass distribution predicted by the reconstructed model is low enough that we can distinguish two models with more than $\sim 2\sigma$ confidence level as well. These results motivate to develop N-body simulations based on different Hubble parameter histories (e.g., introduced the reconstructed model) for more accurate results. However, to compare the suggested probes with observational data, we should consider all the complications raised from the physics of the halo occupation distribution. To find relations between the DM host halos’ statistics and merger history and the luminosity, color, and morphology distribution of the galaxies. We are inspired by an exciting observation [Duncan et al. \(2019\)](#) with Hubble space telescope HST, CANDEL field on

the number of “very near galaxy pairs” as an indication of merging galaxies. We calculate the ratio of the merger rate of DM halos (for two models of Planck-2018 Λ CDM and reconstructed model) in the excursion set theory context in Markov and non-Markov extension. To be more specific, we propose that the merger rate of DM halos is related to the statistics of pair galaxies in the HST, CANDEL Survey. We show decreasing the error bars on the merger rate can distinguish the models with future observations (~ 5 times more accurate data). The better precision can be achieved with better photometric, spectroscopic measurements, and increasing the statistics of galaxies. For future studies, the difference of the number density and merger rate predictions in non-Markov and Markov case should be studied. These differences can be investigated by dark matter N-body simulations. Also, the merger history of DM halos can be studied in the context of excursion set theory of peaks considering the complications of the ellipsoidal collapse. The physics of halo occupation distribution and luminous matter’s bias to dark matter should be reconsidered in the alternative models. We should note that we study the models that differ from Λ CDM only in the Hubble parameter in this scheme. There are theories (e.g., modified gravity) that change the physics of the collapse and the Poisson equation. For this category of models, the non-linear structure formation (collapse models and EST, ...) should be reformulated. Finally, we emphasize that by the upcoming LSS surveys such as Euclid, LSST, WFIRST, ... we will have the opportunity to test models in both background evolution and linear (non-linear) structure formation.

ACKNOWLEDGMENTS

We are grateful to Levon Pogossian, providing us with the reconstructed Hubble parameter data. SB is partially supported by Abdus Salam International Center of Theoretical Physics (ICTP) under the junior associateship scheme. This research is supported by Sharif University of Technology Office of Vice President for Research under Grant No. G960202.

REFERENCES

- Aghanim N. *et al.* [Planck Collaboration], 2018, arXiv:1807.06209 [astro-ph.CO].
 Alam S. *et al.* [BOSS Collaboration], 2017, Mon. Not. Roy. Astron. Soc. **470**, no. 3, 2617.
 Amendola L., 2004, Phys. Rev. D **69**, 103524.
 Ata M. *et al.*, 2018, Mon. Not. Roy. Astron. Soc. **473**, no.4, 4773-4794.
 Baghram S., Movahed M. S. and Rahvar S., 2009, Phys. Rev. D **80**, 064003.
 Baghram S. and Rahvar S., 2010, JCAP **12**, 008.
 Baghram S., Tavasoli S., Habibi F., Mohayae R. and Silk J., 2014, Int. J. Mod. Phys. D **23**, no.12, 1442025.
 Bertschinger E. and Zukin P., 2008, Phys. Rev. D **78**, 024015.
 Baghram S. *et al.*, 2019, Phys. Rev. E **99**, no.6, 062101.
 Bardeen J. M., Bond J. R., Kaiser N. and Szalay A. S., 1986, Astrophys. J. **304**, 15-61.
 Beutler, F. *et al.*, 2011, MNRAS **416** 3017-3032 .
 Betoule M. *et al.*, 2014, Astron. Astrophys. **568**, A22 .

- Bond J. R., Cole S., Efstathiou G. and Kaiser N., 1991, *Astrophys. J.* **379**, 440.
- Bull P. *et al.*, 2016, *Phys. Dark Univ.* **12**, 56-99.
- Camacho H. *et al.* [DES Collaboration], 2019, *Mon. Not. Roy. Astron. Soc.* **487**, no. 3, 3870.
- Cooray A. and Sheth R. K., 2002, *Phys. Rept.* **372**, 1.
- Delubac T. *et al.* [BOSS], 2015, *Astron. Astrophys.* **574**, A59.
- Di Valentino E., Melchiorri A., Mena O. and Vagnozzi S., 2020, *Phys. Dark Univ.* **30**, 100666.
- Di Valentino E., Mukherjee A. and Sen A. A., 2020, [arXiv:2005.12587 [astro-ph.CO]].
- Duncan, K. *et al.*, 2019, *The Astrophysical Journal*, 876(2), 110.
- Eisenstein D. J. and Hu W., 1998, *Astrophys. J.* **496**, 605.
- Font-Ribera A. *et al.* [BOSS], 2014, *JCAP* **05**, 027.
- Gunn J. E. and Gott J. R., 1998, *Astrophys. J.* **176**, 1.
- Heckman T. M. and Best P., 2014, *Ann. Rev. Astron. Astrophys.* **52**, 589-660.
- Hildebrandt H. *et al.*, 2017, *Mon. Not. Roy. Astron. Soc.* **465**, 1454.
- Ishak M., Upadhye A. and Spergel D. N., 2006, *Phys. Rev. D* **74**, 043513 .
- Kameli H. and Baghran S., 2020, *Mon. Not. Roy. Astron. Soc.* **494**, no. 4 , 4907–4913.
- Khosravi N., Baghran S., Afshordi N. and Altamirano N., 2019, *Phys. Rev. D* **99**, no.10, 103526.
- Klypin A. *et al.*, 2020, [arXiv:2006.14910 [astro-ph.CO]].
- Koyama K., 2016, *Rept. Prog. Phys.* **79**, no.4, 046902.
- Maggiore M. and Riotto A., 2010, *Astrophys. J.* **711**, 907-927.
- Maggiore M. and Riotto A., 2010, *Astrophys. J.* **717**, 515-525.
- Man A. and Belli S., 2018, *Nature Astronomy* **2**, no.9, 695.
- Mo, H., Van den Bosch, F., White, S., 2010, *Galaxy formation and evolution*. Cambridge University Press..
- Musso M. and Sheth R. K., 2012, *Mon. Not. Roy. Astron. Soc.* **423**, L102.
- Musso M. and Sheth R. K., 2014, *Mon. Not. Roy. Astron. Soc.* **438**, no. 3, 2683.
- Nikakhtar F. and Baghran S., 2017, *Phys. Rev. D* **96**, no. 4, 043524.
- Nikakhtar F., Ayromlou M., Baghran S., Rahvar S., Rahimi Tabar M. R. and Sheth R. K. , 2018, *Mon. Not. Roy. Astron. Soc.* **478**, no. 4, 5296.
- Paranjape A. and Sheth R. K., 2012, *Mon. Not. Roy. Astron. Soc.* **426**, 2789-2796.
- Peebles P. J. E., 2014, *J. Phys. Conf. Ser.* **484**, 012001.
- Peebles P. J. E., 2020, arXiv:2005.07588 [astro-ph.GA].
- Percival W. J. *et al.* [SDSS], 2010, *Astron. Astrophys. Mon. Not. Roy. Astron. Soc.* **401**, 2148-2168.
- Perlmutter S. *et al.* [Supernova Cosmology Project], 1999, *Astrophys. J.* **517**, 565-586.
- Pogosian L. and Silvestri A., 2008, *Phys. Rev. D* **77**, 023503.
- Poulin V., Smith T. L., Karwal T. and Kamionkowski M., 2019, *Phys. Rev. Lett.* **122**, no.22, 221301.
- Press W. H. and Schechter P. , 1974, *Astrophys. J.* **187**, 425.
- Riess A. G. *et al.*, 1998, *Astron. J.* **116**, 1009-1038.
- Riess A. G., Casertano S., Yuan W., Macri L. M. and Scolnic D., 2019, *Astrophys. J.* **876**, no.1, 85.
- Ross A. J. *et al.*, 2015, *Mon. Not. Roy. Astron. Soc.* **449**, no.1, 835.
- Sheth R. K. and Tormen G., 1999, *Mon. Not. Roy. Astron. Soc.* **308**, 119.
- Sheth R. K. and Tormen G., 2002, *Mon. Not. Roy. Astron. Soc.* **329**, 61.
- Tinker J. L., Kravtsov A. V., Klypin A., Abazajian K., Warren M. S., Yepes G., Gottlobler S. and Holz D. E., 2008, *Astrophys. J.* **688**, 709-728.
- Wang Y. *et al.* [BOSS], 2017, *Mon. Not. Roy. Astron. Soc.* **469**, no.3, 3762-3774 .
- Wang Y., Pogosian L., Zhao G. B. and Zucca A., 2018, *Astrophys. J. Lett.* **869**, L8.
- Zentner A. R., 2007, *Int. J. Mod. Phys. D* **16**, 763.

This paper has been typeset from a $\text{\TeX}/\text{\LaTeX}$ file prepared by the author.